Structure of the Cobalt-Dependent Methionine Aminopeptidase from *Escherichia coli*: A New Type of Proteolytic Enzyme‡

Steven L. Roderick§ and Brian W. Matthews*

Institute of Molecular Biology, Howard Hughes Medical Institute, and Department of Physics, University of Oregon, Eugene, Oregon 97403

Received November 24, 1992

ABSTRACT: The X-ray structure of *Escherichia coli* methionine aminopeptidase (MAP) has been determined to 2.4-Å resolution and refined to a crystallographic *R*-factor of 18.2%. The fold is novel and displays internal pseudo-2-fold symmetry which structurally relates the first and second halves of the polypeptide chain. The topology consists of a central antiparallel β-sheet covered on one side by two pairs of α-helices and by a C-terminal loop. The other face of the β-sheet, together with some irregular loops, forms the active site, which contains two cobalt ions 2.9 Å apart. These metal ions are liganded by the side chains of Asp 97, Asp 108, Glu 204, Glu 235, and His 171 with approximate octahedral coordination. In terms of both the novel backbone fold and the constitution of the active site, MAP appears to represent a new class of proteolytic enzyme.

Although most proteins are synthesized beginning with either methionine or formylmethionine, this residue is often absent from the NH_2 terminus of mature polypeptides (Flinta et al., 1986). In prokaryotes and organelles, the *N*-formyl group of the initiator methionine is removed by a deformylase. The amino-terminal leader methionine residue may then be cleaved by a methionine aminopeptidase (MAP) on the basis of the identity of the adjacent residue. The resulting NH_2-terminal residue may then be subject to additional covalent modifications such as N-acetylation or N-myristoylation. The structure of the mature NH_2 terminus plays a role in N-directed degradation pathways (Ben-Bassat & Bauer, 1987; Gonda et al., 1989; Hershko, 1991; Tobias et al., 1991) and in targeting to cellular membranes (Towler et al., 1988).

Methionine aminopeptidases (MAP) have been studied in *Escherichia coli* (Ben-Bassat et al., 1987), *Salmonella typhimurium* (termed pepM) (Miller et al., 1987; Wingfield et al., 1989), yeast (Chang et al., 1990, 1992), and porcine liver (Kendall & Bradshaw, 1992). Preparations from several of these sources demonstrate that MAP is a soluble monomer with pH optimum near neutrality and a metalloenzyme maximally stimulated by Co^{2+}. The identity of the metal ion bound in vivo has not, however, been firmly established. Deletion of the gene encoding MAP is lethal in *E. coli* and *S. typhimurium*, but not in yeast (Chang et al., 1989, 1992; Miller, C. G., et al., 1989).

The substrate specifity of these enzymes is generally consistent with the distribution of N-terminal sequences obtained from natural and site-directed mutant proteins (Huang et al., 1987; Tsunasawa et al., 1987; Boissel et al., 1988; Arfin & Bradshaw, 1988; Hirel et al., 1989). Favored substrates for MAP are those which possess an NH_2-terminal methionine adjacent to a physically small residue.

The prokaryotic and yeast MAP genes have been sequenced, and they display a significant degree of amino acid sequence identity. Although the prokaryotic MAPs display no significant amino acid sequence homology to any other protein, the MAP from yeast contains an NH_2-terminal extension of ~120 residues relative to the prokaryotic forms. This extension contains sequences similar to Cys-Cys and Cys-His zinc-finger domains and has been suggested to interact with ribosomes, allowing for cotranslational excision of the leader methionine residue (Chang et al., 1992).

We have undertaken an X-ray crystallographic study of the MAP from *E. coli* in order to understand the means by which this enzyme utilizes Co^{2+}, the basis for its substrate specificity, and to study the structure and function of aminopeptidases in general. The MAP from *E. coli* is a monomeric enzyme with a calculated molecular weight of 29 333. It has been overproduced, purified, and crystallized (Ben-Bassat et al., 1987; Roderick & Matthews, 1988). We present here the overall polypeptide chain fold and active site geometry resulting from a 2.4-Å X-ray crystallographic study.

MATERIALS AND METHODS

Purification and Crystallization. The methionine aminopeptidase from *E. coli* was cloned, overproduced, and purified as previously described (Ben-Bassat et al., 1987). Crystallization was carried out by a modification of a previously published procedure (Roderick & Matthews, 1988). A solution of 42 mg/mL protein, 25 mM sodium cacodylate, pH 6.8, 25 mM K_2SO_4, 100 mM NaCl, and 1 mM $CoCl_2$ was mixed with an equal volume of 14% (w/v) polyethylene glycol 4000 and 0.5% (w/v) octyl β-glucoside. A 15-μL drop of this solution was transferred to a siliconized coverslip and inverted over a reservoir containing 0.5 mL of 23–35% polyethylene glycol 4000. Crystals were inspected after 5 days and harvested into a storage solution containing 25% polyethylene glycol 4000, 25 mM sodium cacodylate, pH 6.5, 25 mM K_2SO_4, 100 and mM NaCl, 10 mM L-methionine, and 1 mM $CoCl_2$.

These crystals belong to space group $P2_1$ with unit cell parameters a = 39.0 Å, b = 61.7 Å, c = 54.5 Å, and β = 107.3°. The largest crystals typically attain a size of 0.6 × 0.4 × 0.3 mm and display a layered appearance perpendicular to the crystal b-direction. Bragg reflections extend to 2.1 Å in the a^*-direction but only to about 2.5 Å in the b^*- and c^*-directions. These crystals remain ordered in the X-ray beam for about 36 h at room temperature.

‡ The coordinates and structure factors of this protein have been deposited in the Brookhaven Protein Data Bank under the file names 1MAT and 1MAT-SF, respectively.

* To whom correspondence should be addressed.

§ Present address: Department of Biochemistry, Albert Einstein College of Medicine, 1300 Morns Park Ave., Bronx, NY 10461.

0006-2960/93/0432-3907$04.00/0 © 1993 American Chemical Society

Data Measurement and Primary Phasing. Primary phases were determined by the method of isomorphous replacement using four heavy atom derivatives. Heavy atom positions were initially located with 5.0-Å-resolution data measured with an Enraf-Nonius CAD4 diffractometer. Data to 2.4-Å resolution were measured from single crystals with a San Diego Multiwire (Xuong et al., 1988) area detector using graphite monochromated X-rays generated by a Rigaku RU200 rotating anode generator. These data were divided into time-dependent parcels for scaling by using linear and exponential scale factors and merged with the diffractometer data to create the final data sets. The derivative crystal preparation schemes and diffraction data measurement statistics are summarized in Table I.

Heavy atom parameter refinement using isomorphous and anomalous scattering data was carried out with the program HEAVY (Terwilliger & Eisenberg, 1983) using traditional lack-of-closure residuals, which yielded the heavy atom parameters and statistics presented in Table II. Parallel refinements were also conducted with the PROTEIN program package (Steigemann, 1974). Of the four heavy atom derivatives used, only the thallium acetate derivative was of good quality. The mean figure-of-merit for the phase determination to 2.5-Å resolution was 0.61.

Model Building and Refinement. Electron density maps were calculated at 2.5- and 2.8-Å resolution by using phase sets derived from the HEAVY- and PROTEIN-based heavy atom parameter refinements. These maps were similar but were inspected throughout the model building procedure due to small but significant differences between them. The maps were modeled by using the graphics programs FRODO and TOM operating on Evans and Sutherland PS330 and ESV graphics devices (Jones & Thirup, 1986). Atomic models were refined by using the restrained least squares method as implemented in the TNT refinement program package and employing the "conjugate direction" parameter shift method (Tronrud et al., 1987; Tronrud, 1992). Phases obtained from intermediate models were combined with the isomorphous replacement phases for calculation of $2F_o - F_c$ maps. Difficult regions of the map were reinspected with refine/omit maps.

The current atomic model includes four overall anisotropic scale parameters, a two-parameter disordered solvent model, neighbor-restrained thermal parameters, 15 solvent molecules, atoms corresponding to residues 2–264 of the enzyme, and the active site cobalt ions. The *R*-factor for 8387 reflections (82% complete) from 52- to 2.4-Å resolution is 18.2% with root-mean-square deviations of bond lengths and angles from ideality of 0.019 Å and 2.9°. A Ramachandran plot of the main-chain torsion angle pairs is shown in Figure 1.

RESULTS AND DISCUSSION

Polypeptide Chain Fold. Stereoviews of ribbon and α-carbon diagrams of *E. coli* methionine aminopeptidase corresponding to residues 2–264 and the active site cobalt ions are shown in Figure 2. Consistent with the substrate specificity for this enzyme, no electron density is seen for an NH_2-terminal methionine (adjacent residue alanine). The overall shape of the molecule is cylindrical with radius 22 Å and height 25 Å. A curved antiparallel β-sheet is centrally located, with one face covered by the C-terminal 21 residues and four α-helices. The other side of this sheet is partially covered by loops inserted between these elements of secondary structure. Two cobalt ions are bound in the central part of the sheet. None of the seven cysteine residues present in the sequence of *E. coli* MAP participate in disulfide bridges.

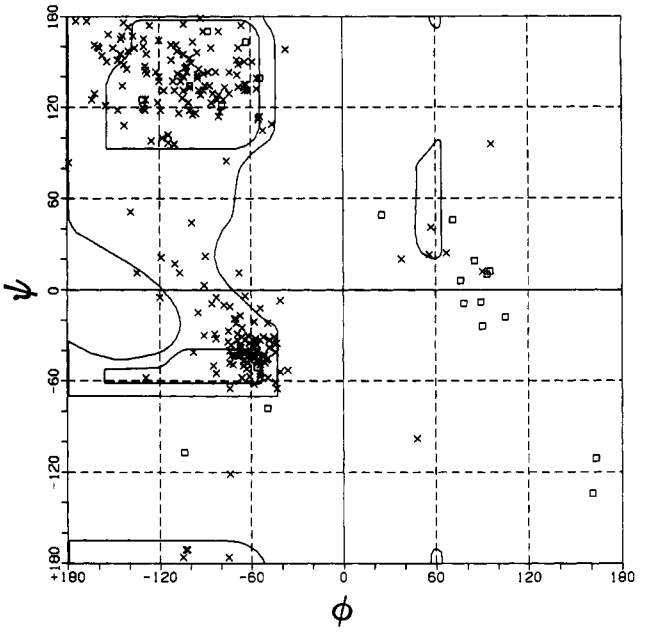

FIGURE 1: Ramachandran diagram (Ramachandran et al., 1963) of main-chain torsion angle pairs φ and ψ for the refined model of methionine aminopeptidase. Glycine residues are indicated by squares (□), and non-glycines, by crosses (×).

Internal 2-fold Symmetry. On closer inspection, it is apparent that two of the β-strands and the helix–bend–helix motif contained in the first half of the sequence (residues 11–116) are closely related to similar structures in the second half (residues 120–241). The least squares transformation, which superimposes 64 selected α-carbon atoms from the second half of the sequence on those of the first half, is equivalent to a rotation of 174° and a translation of just 0.6 Å parallel to the axis of rotation. The axis passes 4 Å below the midpoint of the two cobalt ions and is oriented nearly perpendicular to the plane of the page in Figure 2. The superimposed α-carbon atoms resulting from this transformation are shown in Figure 3.

Structurally similar domains within a single polypeptide chain are a characteristic of two other classes of protease, namely, the chymotrypsin-like serine proteases (Blow, 1969; McLachlan, 1979) and the acid proteases (Subramanian et al., 1977; Miller, M., et al., 1989). In both of these cases, as with MAP, the active site is located at the junction of the two domains. Pronounced structural correspondence between two structural domains formed by a single polypeptide chain has been observed for other proteins as well, for example, rhodanese (Ploegman et al., 1978), and has often been taken as evidence of an ancestral gene duplication and fusion. In the present case, the relationship between the two halves is nearly equivalent to a pure 2-fold rotation and is consistent with an ancestral duplication/fusion of a gene which once coded for subunits of a dimer [cf. Miller, M., et al. (1989)]. After duplication, the sequences of these genes could then diverge through independent evolution, either before or after gene fusion. Although such a scheme could result in retention of apparent sequence and structural homology between the two halves, the observed level of sequence identity determined from the structurally defined superposition, as shown in Figure 4, is rather limited (19%; 12/64 pairs).

As is usually the case, the structural relationship between the two halves appears to be much better conserved than the sequence correspondence. The internal 2-fold rotation axis relates the 64 selected α-carbon pairs with a root-mean-square

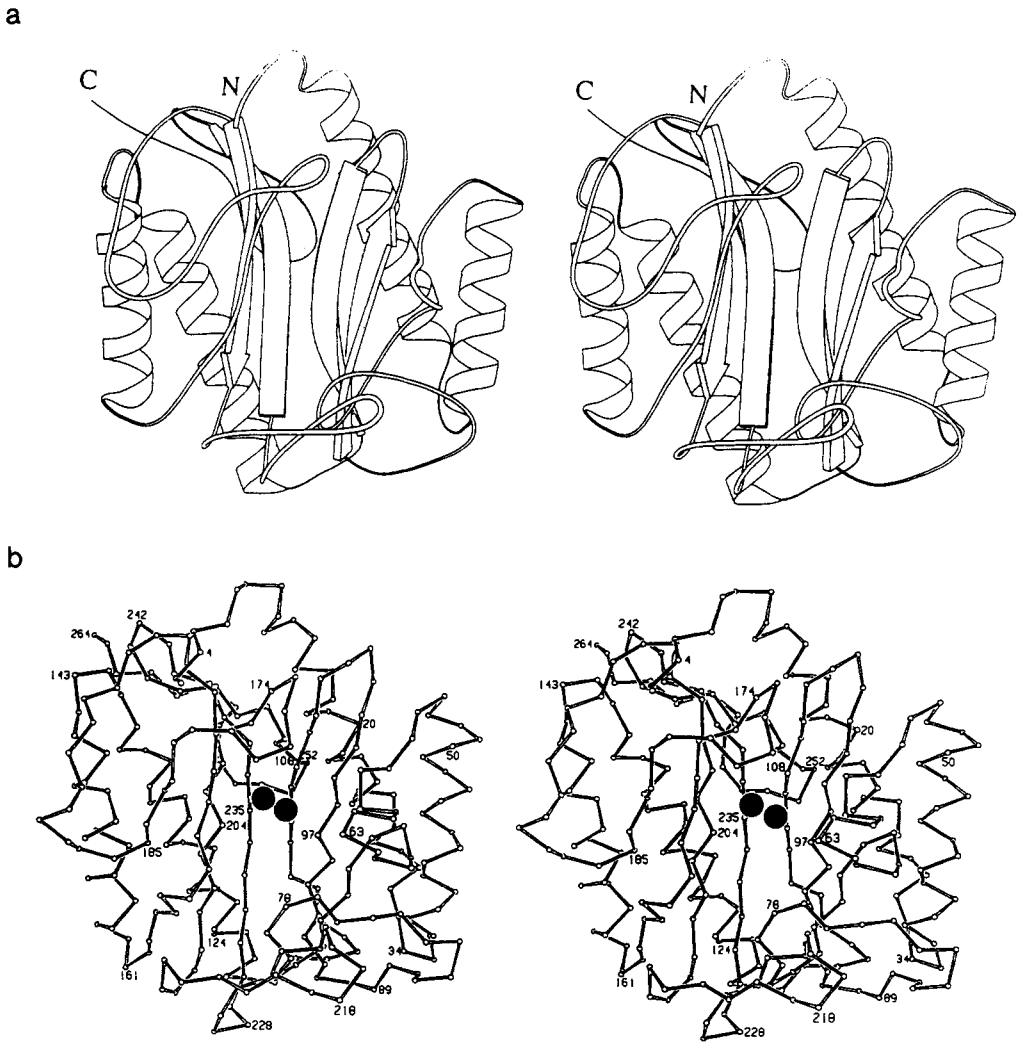

FIGURE 2: Overall polypeptide chain fold of methionine aminopeptidase. The viewing direction is similar in both diagrams and is approximately parallel to the internal 2-fold rotation axis. (a) Schematic diagram produced by the program RIBBON (Priestle, 1988). (b) Stereoview of the α-carbon atoms, including the two active site cobalt ions (Co1, left; Co2, right).

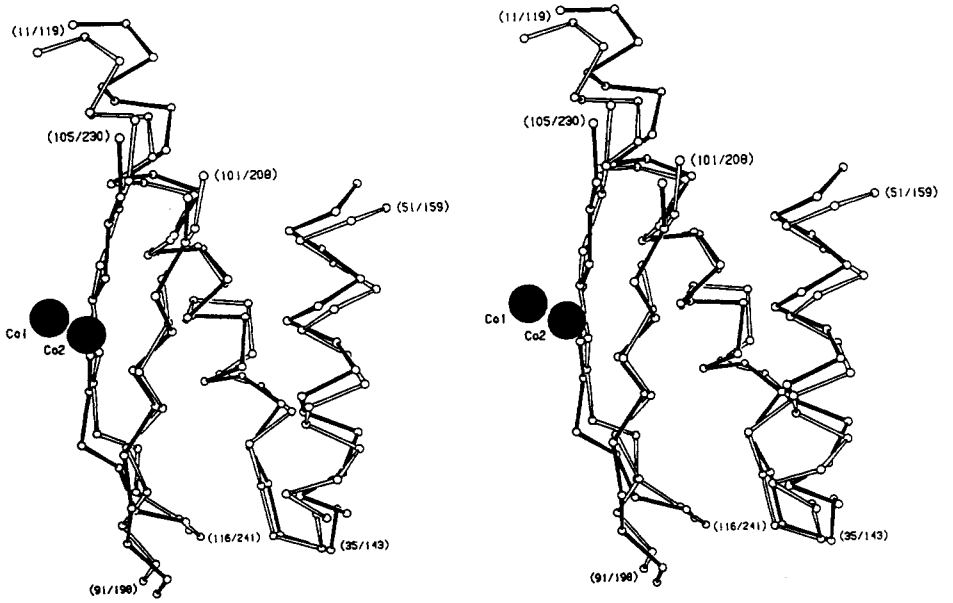

FIGURE 3: Stereoview of 64 selected α-carbon atoms from the second half of the amino acid sequence (dark bonds) superimposed by the internal 2-fold rotation axis on equivalent residues in the first half (open bonds). Equivalent residue numbers are indicated in parentheses (see Figure 4). The untransformed active site cobalt ions (i.e., aligned relative to the amino-terminal domain) are shown for comparison.

discrepancy of 1.4 Å (Figure 3). Least squares superposition of the contiguous 41 α-carbon atoms of each helix–bend–helix motif (residues 11–51 or 119–159) separately with each contiguous 41-α-carbon segment from every protein structure

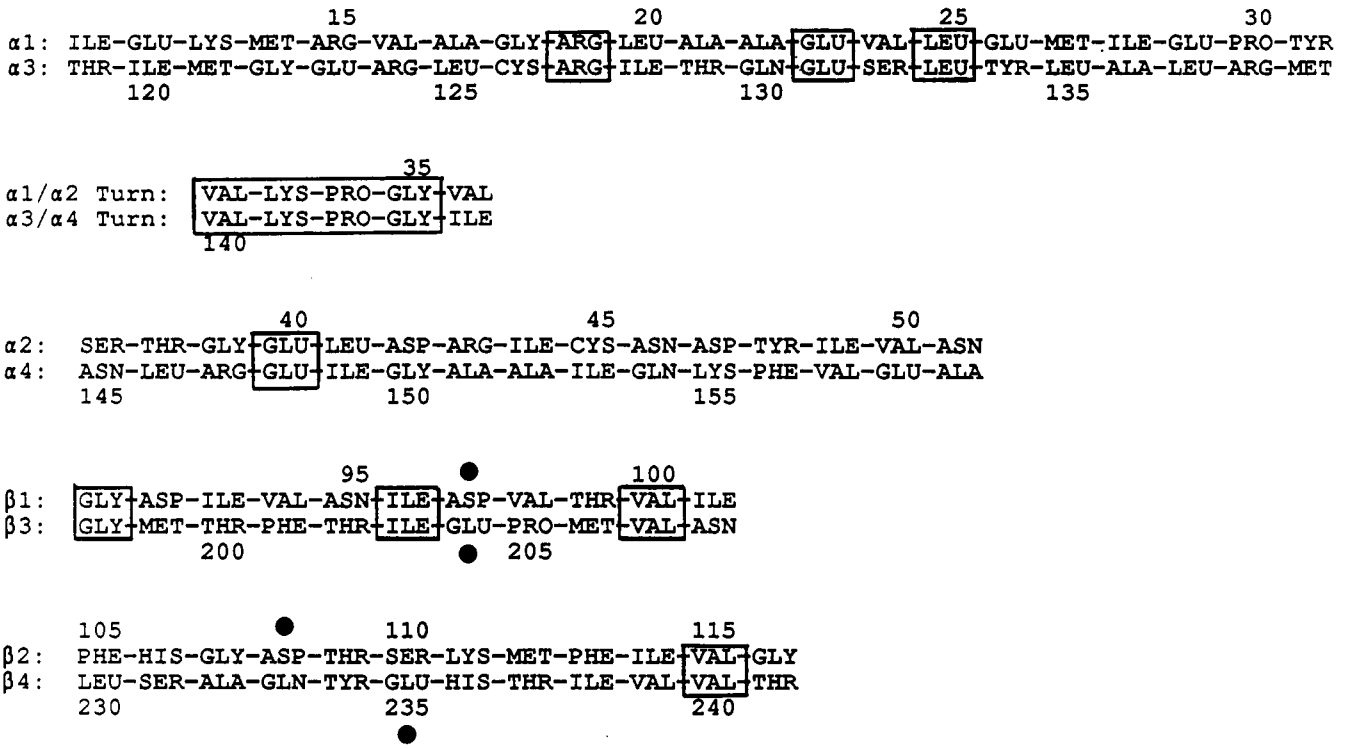

FIGURE 4: Structurally defined amino acid sequence alignment of the 64 selected residue pairs. The secondary structural element is indicated to the left. Identical residues are boxed. Residues donating ligands to the cobalt ions are marked (●).

in the Brookhaven Protein Data Bank[1] (Bernstein et al., 1977) revealed no comparably good superpositions. In addition, the superposition of the (noncontiguous) MAP β-strands and helix–bend–helix motifs on one another preserves the relative polarity of the sequence within each piece of secondary structure as well as the sequential order of these pieces within each half. These observations strongly support the idea of a homologous relationship between the first and second halves of the methionine aminopeptidase sequence based on the ancestral gene duplication/fusion event.

About 50% of the α-carbons in the MAP structure are closely related in pairs by the 2-fold symmetry. The remaining residues, which are not as closely related, include the NH_2- and C-terminal segments of 10 and 21 residues, respectively, and four segments ranging in length from 3 to 38 residues which are inserted in topologically related gaps. Three of these segments fold toward the face of the central β-sheet which binds the active site cobalt ions (Figure 2). The largest two segments, residue ranges 52–90 and 160–197, are of different lengths but are inserted in related gaps and share topological similarity (Figure 2).

Active Site. The active site contains two cobalt atoms, termed Co1 and Co2, bound to the center of the central β-sheet and separated by 2.9 Å. The internal 2-fold symmetry of the backbone does not relate the cobalt atoms. Rather, the symmetry axis passes about 4 Å below the midpoint of the two ions (Figure 2).

The distance between the cobalt ions of MAP is somewhat larger than twice the covalent radius for cobalt (2.32 Å) and is similar to the distance between the binuclear zinc atoms of leucine aminopeptidase (Zn^{2+}/Zn^{2+}; 2.9 Å) (Burley et al., 1990). However, the separation is significantly shorter than that between the metal ions of alkaline phosphatase (Zn^{2+}/Zn^{2+}; 3.9 Å) (Sowadski et al., 1985), P1 nuclease (Zn^{2+}/Zn^{2+}; 3.2 Å) (Volbeda et al., 1991), phospholipase C (Zn^{2+}/Zn^{2+}; 3.3 Å) (Hough et al., 1989), DNA polymerase I (Zn^{2+}/Mg^{2+}; 3.9 Å) (Beese & Steitz, 1991), xylose isomerase (Mn^{2+}/Mn^{2+}; 4.9 Å) (Whitlow et al., 1991), and concanavalin A (Mn^{2+}/Ca^{2+}; 4.3 Å) (Hardman et al., 1982).

[1] X.-J. Zhang, unpublished program EDPDB.

Table I: Data Measurement Statistics[a]

	resolution (Å)	observations	completeness of data	R_{Merge}	R_{iso}
native	2.5	8054	0.93	0.035	
demetalized[b]	3.0	4763	0.95	0.060	0.162
samarium chloride[c]	3.0	4739	0.94	0.058	0.153
trimethyllead acetate[d]	2.5	7848	0.91	0.047	0.137
thallium acetate[e]	2.5	7601	0.88	0.035	0.130

[a] $R_{merge} = \sum\sum|I_{hkl,i} - \langle I_{hkl}\rangle| / \sum|I_{hkl,i}|$ for all data, $I_{hkl,i}$ being an individual intensity measurement. $R_{iso} = \sum||F_{hkl,native}| - |F_{hkl,derivative}|| / \sum|F_{hkl,native}|$ for all data. [b] Demetalized crystals were prepared by soaking native crystals in a storage solution lacking $CoCl_2$ and containing 10 mM EDTA for 3 days. [c] Prepared from demetalized crystals by soaking in a storage solution lacking K_2SO_4 and $CoCl_2$ and containing 5 mM $SmCl_3$ for 3 days. [d] Soak of 5 mM for 3 days (Holden & Rayment, 1991). [e] Soak of 5 mM for 2 days. All soaks and data measurements were carried out at ambient temperature.

It appears that the cobalt ions bound to methionine aminopeptidase are present at equal occupancy and have similar thermal mobility. Crystallographic refinement of the holoenzyme relative to the demetalized form suggests that the cobalt ions have occupancies close to unity (Tables I and II). In this refinement the thermal factors of the two cobalts were set at 25 $Å^2$. Conversely, if the occupancies were set to unity, the refined thermal factors were also very similar, 27 $Å^2$ for Co1 and 29 $Å^2$ for Co2. This correspondence for the cobalt atoms of MAP is in contrast to significantly different thermal factors determined for the zinc atoms of leucine aminopeptidase (13 and 38 $Å^2$) (Burley et al., 1991, 1992).

The cobalt ions of MAP are coordinated nonequivalently by the side-chain atoms of Asp 97, Asp 108, Glu 204, Glu

Table II: Heavy Atom Parameter Refinement and Phase Calculation Statistics[a]

derivative	site	occupancy	X	Y	Z	$R_{centric}$[b]	$\langle f_H \rangle / E$[c]
demetalized	Co1	-0.92	0.1464	0.0069	0.2066	0.70	1.06
	Co2	-1.04	0.1394	-0.0069	0.1529		
samarium chloride	Co1	-0.79	0.1464	0.0069	0.2066	0.68	0.97
	Co2	-0.85	0.1394	-0.0069	0.1529		
	Sm1	0.53	0.1377	-0.0038	0.2035		
	Sm2	0.43	0.1275	-0.0138	0.1625		
trimethyllead acetate	Pb1	0.56	-0.0044	0.0181	0.2217	0.62	1.06
	Pb2	0.30	0.0145	-0.0483	0.1823		
thallium acetate	Tl1	0.80	0.7833	0.3692	0.5977	0.36	1.77
mean figure-of-merit = 0.61							

[a] Heavy atom parameters and phasing statistics were calculated with HEAVY, using Co^{2+}-containing crystal data as the native data set. The occupancy values are on an approximate scale and were determined with thermal factors set to 25 Å^2. Negative occupancies indicate the absence of an atom relative to the native enzyme. The positional parameters for the cobalt atoms in the samarium chloride derivative were held constant at values determined for the demetalized derivative. The two samarium sites are separated by 2.2 Å and are present at nearly half occupancy, indicating that these sites occupy mutually exclusive positions. [b] $R_{centric} = \Sigma||f_{H(obsd)}| - |f_{H(calcd)}||/\Sigma|f_{H(obsd)}|$ for centric reflections. [c] $\langle f_H \rangle$ is the rms heavy atom scattering. E is the rms lack of closure calculated at the centroid phase angle.

Table III: Cobalt–Ligand Distances (Å)

ligand	Co1	Co2	ligand	Co1	Co2
Asp 97 $O^{\delta 1}$		2.2	Glu 204 $O^{\epsilon 2}$	1.6	
Asp 97 $O^{\delta 2}$		2.0	Glu 235 $O^{\epsilon 1}$		2.1
Asp 108 $O^{\delta 1}$		2.0	Glu 235 $O^{\epsilon 2}$	2.3	
Asp 108 $O^{\delta 2}$	2.0		Co1		2.9
His 171 $N^{\epsilon 2}$	2.1		Co2	2.9	

235, and His 171. Both cobalt atoms accept ligands from each half of the enzyme. The four acidic residues extend from each of the longest four β-strands of the central antiparallel β-sheet. Although these strands are related by the internal 2-fold axis, the only metal ligands related by this transformation are Asp 97 and Glu 204 (Figure 4). The five residues involved in coordinating the metal atoms are conserved in a recent amino acid sequence alignment of four MAP sequences, with the exception of Glu 235, which is glutamine in *Bacillus subtilis* MAP (Chang et al., 1992).

The cobalt–ligand distances are given in Table III, and the coordination is illustrated in Figure 5. Although some question remains concerning the conformation of the side chain of Glu 235 due to electron density of poor quality, the orientation of the oxygen ligands to the cobalt ions is clearly syn for Asp 97 and Asp 108. His 171 interacts with Co1 through its imidazole $N^{\epsilon 2}$ atom (2.1 Å) and donates a hydrogen bond from $N^{\delta 1}$ to the carbonyl oxygen of Gly 172 (2.6 Å). This arrangement is similar to the carbonyl–histidine–metal interactions found in many zinc proteins and has been explained in terms of promoting metal ion interaction due to ligand orientation effects (Kester & Matthews, 1977) and modulation of histidine basicity toward the metal ion (Christianson & Alexander, 1989).

The protein–cobalt and cobalt–cobalt interactions for each cobalt atom are arrayed in approximate octahedral geometry, as is frequently observed in cobalt-containing complexes (Cotton & Wilkinson, 1980). The two cobalt and six equatorial ligand atoms are very nearly coplanar, with a root-mean-square discrepancy from the least squares plane of 0.3 Å.

Although we have not yet located an inhibitor bound to the active site of MAP, it is clear that only a single sterically accessible cavity is available for substrate to bind near the cobalt atoms. Electron density in this region does not suggest the presence of L-methionine, present in the crystal storage solution at 10 mM concentration, but does tentatively suggest that solvent molecules may be bound to Co1 and Co2 in the direction of the "absent" octahedral ligands (Figure 5). These solvent molecules would be in a position to form hydrogen bonds to the $N^{\epsilon 2}$ atom of His 178 or the $O^{\gamma 1}$ atom of Thr 99 (Figure 5).

Adjacent to the metal binding site is a closed pocket lined by the side chains of Cys 59, Cys 70 (S–S distance 4.4 Å), Tyr 62, Tyr 65, Phe 177, and Trp 221. This hydrophobic pocket provides the major binding site for the amphipathic trimethyllead ion used as a heavy atom derivative (atom Pb1; Table II). This is the most obvious candidate for the binding site of the amino-terminal methionine side chain required for substrate recognition and catalysis.

Although the two aminopeptidases with defined three-dimensional structure, the leucine aminopeptidase from bovine lens (LAP) (Burley et al., 1992) and the *E. coli* methionine aminopeptidase reported here, share similarities in endoproteolytic specificity and their use of binuclear metal ions at the active site, it should be emphasized that these enzymes are also significantly different. The LAP is a large hexameric enzyme, whereas the MAP from *E. coli* is a much smaller internally symmetric monomer. The two aminopeptidases

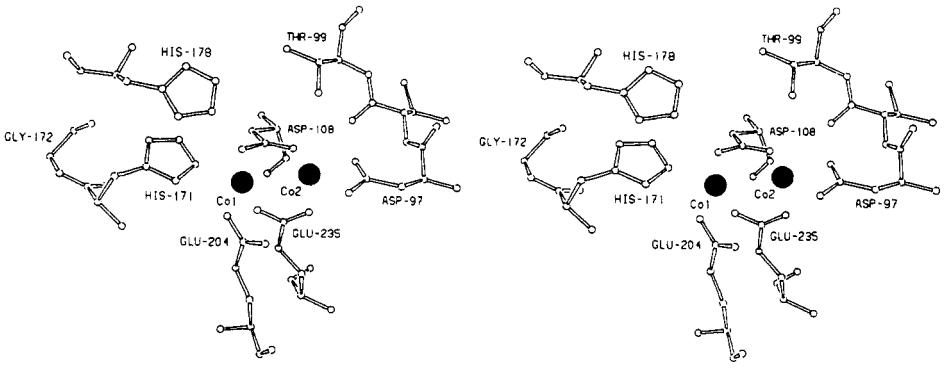

FIGURE 5: Stereoview of the active site including cobalt ions and protein ligands.

have no noticeable amino acid sequence homology or structural similarity of their polypeptide chain folds. The zinc ions in LAP bind near the edge of a mixed β-sheet, while the cobalt ions of MAP bind at the center of an antiparallel sheet. Although the ligands of the positively charged active site metal ions in both proteases necessarily include acidic residues, the overall arrangement of ligands in MAP is octahedral and makes use of a histidine residue as the sole nonacidic protein ligand rather than a lysine residue as in the case of LAP. The active site of LAP includes Lys 262 and Arg 336 (Burley et al., 1992), whereas the active site of MAP contains neither lysine nor arginine, but does include a histidine. For these reasons, we believe that these two aminopeptidases are evolutionarily distinct and that the methionine aminopeptidase represents a new type of proteolytic enzyme.

ACKNOWLEDGMENT

We are grateful to N. Jung, K. Bauer, L. Konno, R. Drummond, and S. Chang, previously of Cetus Corp., for helpful discussions concerning this project and for providing purified methionine aminopeptidase and the expression system. We would also like to acknowledge the help and advice of Drs. L. Weaver, D. Tronrud, S. J. Remington, and R. DuBose in data collection and computational aspects.

REFERENCES

Arfin, S., & Bradshaw, R. A. (1988) *Biochemistry 27*, 7979–7984.
Beese, L. S., & Steitz, T. A. (1991) *EMBO J. 10*, 25–33.
Ben-Bassat, A., & Bauer, K. (1987) *Nature 326*, 315.
Ben-Bassat, A., Bauer, K., Chang, S.-Y., Myambo, K., Boosman, A., & Chang, S. (1987) *J. Bacteriol. 169*, 751–757.
Bernstein, F. C., Koetzle, T. F., Williams, G. J. B., Meyer, E. F., Brice, M. D., Rodgers, J. R., Kennard, O., Shimanouchi, T., & Tasumi, M. (1977) *J. Mol. Biol. 112*, 535–542.
Blow, D. M. (1969) *Biochem. J. 112*, 261–268.
Boissel, J.-P., Kasper, T. J., & Bunn, H. F. (1988) *J. Biol. Chem. 263*, 8443–8449.
Burley, S. K., David, P. R., Taylor, A., & Lipscomb, W. N. (1990) *Proc. Natl. Acad. Sci. U.S.A. 87*, 6878–6882.
Burley, S. K., David, P. R., & Lipscomb, W. N. (1991) *Proc. Natl. Acad. Sci. U.S.A. 88*, 6916–6920.
Burley, S. K., David, P. R., Sweet, R. S., Taylor, A., & Lipscomb, W. N. (1992) *J. Mol. Biol. 224*, 113–140.
Chang, S.-Y. P., McGary, E. C., & Chang, S. (1989) *J. Bacteriol. 171*, 4071–4072.
Chang, Y.-H., Teichert, U., & Smith, J. A. (1990) *J. Biol. Chem. 265*, 19892–19897.
Chang, Y.-H., Teichert, U., & Smith, J. A. (1992) *J. Biol. Chem. 267*, 8007–8011.
Christianson, D. W., & Alexander, R. S. (1989) *J. Am. Chem. Soc. 111*, 6412–6419.
Cotton, F. A., & Wilkinson, G. (1980) *Advanced Inorganic Chemistry*, 4th ed., p 768, John Wiley and Sons, New York.
Flinta, C., Persson, B., Jornvall, H., & von Heijne, G. (1986) *Eur. J. Biochem. 154*, 193–196.
Gonda, D. K., Bachmair, A., Wunning, I., Tobias, J. W., Lane, W. S., & Varshavsky, A. (1989) *J. Biol. Chem. 264*, 16700–16712.
Hardman, K. D., Agarwal, R. C., & Freiser, M. J. (1982) *J. Mol. Biol. 157*, 69–86.
Hershko, A. (1991) *Trends Biochem. Sci. 16*, 265–268.
Hirel, Ph.-H., Schmitter, J.-M., Dessen, P., Fayat, G., & Blanquet, S. (1989) *Proc. Natl. Acad. Sci. U.S.A. 86*, 8247–8251.
Holden, H. M., & Rayment, I. (1991) *Arch. Biochem. Biophys. 291*, 187–194.
Hough, E., Hansen, L. K., Birknes, B., Jynge, K., Hansen, S., Hordvik, A., Little, C., Dodson, E., & Derewenda, Z. (1989) *Nature 338*, 357–360.
Huang, S., Elliot, R. C., Liu, P.-S., Koduri, R. K., Weickmann, J. L., Lee, J.-H., Blair, L. C., Ghosh-Dastidar, P., Bradshaw, R. A., Bryan, K. M., Einarson, B., Kendall, R. L., Kolacz, K. H., & Saito, K. (1987) *Biochemistry 26*, 8242–8246.
Jones, T. A., & Thirup, S. (1986) *EMBO J. 5*, 819–822.
Kendall, R. L., & Bradshaw, R. A. (1992) *J. Biol. Chem. 267*, 20667–20673.
Kester, W. R., & Matthews, B. W. (1977) *Biochemistry 16*, 2506–2516.
McLachlan, A. D. (1979) *J. Mol. Biol. 128*, 49–79.
Miller, C. G., Strauch, K. L., Kukral, A. M., Miller, J. L., Wingfield, P. T., Mazzei, G. J., Werlen, R. C., Graber, P., & Movva, N. R. (1987) *Proc. Natl. Acad. Sci. U.S.A. 84*, 2718–2722.
Miller, C. G., Kukral, A. M., Miller, J. L., & Movva, N. R. (1989) *J. Bacteriol. 171*, 5215–5217.
Miller, M., Jaskolski, M., Rao, J. K. M., Leis, J., & Wlodawer, A. (1989) *Nature 337*, 576–579.
Ploegman, J. H., Drent, G., Kalk, K. H., & Hol, W. G. J. (1978) *J. Mol. Biol. 123*, 557–594.
Priestle, J. (1988) *J. Appl. Crystallogr. 21*, 572–576.
Ramachandran, G. N., Ramakrishnan, C., & Sasisekharan, V. (1963) *J. Mol. Biol. 7*, 95–99.
Roderick, S. L., & Matthews, B. W. (1988) *J. Biol. Chem. 263*, 16531.
Sowadski, J. M., Handschumacher, M. D., Murthy, H. M. K., Foster, B. A., & Wyckoff, H. W. (1985) *J. Mol. Biol. 186*, 417–433.
Steigemann, W. (1974) Ph.D. Thesis, Technische Universität München.
Subramanian, E., Swan, I. D. A., Liu, M., Davies, D. R., Tickle, I. J., & Blundell, T. L. (1977) *Proc. Natl. Acad. Sci. U.S.A. 74*, 556–559.
Terwilliger, T. C., & Eisenberg, D. (1983) *Acta Crystallogr. A39*, 813–817.
Tobias, J. W., Shrader, T. E., Rocap, G., & Varshavsky, A. (1991) *Science 254*, 1374–1377.
Towler, D. A., Gordon, J. I., Adams, S. P., & Glaser, L. (1988) *Annu. Rev. Biochem. 57*, 69–99.
Tronrud, D. E. (1992) *Acta Crystallogr. A48*, 912–916.
Tronrud, D. E., Ten Eyck, L. F., & Matthews, B. W. (1987) *Acta Crystallogr. A43*, 489–503.
Tsunasawa, S., Stewart, J. W., & Sherman, F. (1985) *J. Biol. Chem. 260*, 5382–5391.
Volbeda, A., Lahm, A., Sakiyama, F., & Suck, D. (1991) *EMBO J. 10*, 1607–1618.
Whitlow, M., Howard, A. J., Finzel, B. C., Poulos, T. L., Winbourne, E., & Gilliland, G. L. (1991) *Proteins: Struct., Funct., Genet. 9*, 153–173.
Wingfield, P., Graber, P., Turcatti, G., Movva, N. R., Pelletier, C. S., Rose, K., & Miller, C. G. (1989) *Eur. J. Biochem. 180*, 23–32.
Xuong, N. H., Nielsen, C. H., Hamlin, R., & Anderson, D. (1985) *J. Appl. Crystallogr. 181*, 342–350.